

## Supporting Information

### Molecular Engineering of Two-dimensional Hybrid Perovskites with Broadband Emission for White Light-emitting Diodes

Hongwei Hu,<sup>a</sup> Samuel A. Morris,<sup>a</sup> Xianfeng Qiao,<sup>b</sup> Daming Zhao,<sup>c</sup> Teddy Salim,<sup>a</sup> Bingbing Chen,<sup>a</sup> Elbert E. M. Chia,<sup>c</sup> and Yeng Ming Lam<sup>\*a</sup>

#### Experimental details

##### Material and synthesis

PbBr<sub>2</sub> (99.999%) was purchased from TCI. Unless otherwise noted, all reagents were purchased from Sigma-Aldrich, Merck.

**Methoxybenzylammonium bromides** was synthesized by adding HBr (48wt% in water) into 2-methoxybenzylamine, 3-methoxybenzylamine, or 4-methoxybenzylamine in ethanol at 0 °C (molar ratio of amine to HBr = 1:1.2). The crude product was obtained by slowly evaporating the solvent under reduced pressure. Then the white precipitate was dissolved in ethanol and recrystallized by slowly adding diethyl ether. The small crystals were further washed with diethyl ether several times before drying them in vacuum oven. After drying overnight, they were all sealed under nitrogen and transferred into a nitrogen-filled glove box for further use.

**Single crystals** were grown from precursor solution (in anhydrous dimethylformamide) in stoichiometric ratio of the organic cations and PbBr<sub>2</sub>. Slow evaporation of the solvent in several days afforded small crystal pallets suitable for single-crystal characterization.

**Thin film samples** were prepared by spin-coating of the precursor solution on precleaned glass substrates, followed by annealing at 120 °C for 30 min. Powder samples were prepared by dropping the precursor solution into toluene with 1 to 10 volume ratios. Precipitates were collected and completely dried inside glovebox.

**Mesoporous silica** was synthesized using the reported method.<sup>1</sup> After washing in diluted HCl for several times, the mesoporous silica (Meso-SiO<sub>2</sub>) was dried in oven at 70 °C for 24 h before transferring into glove box. It was further dried at 150 °C inside the glove box for overnight. Perovskite implanted Meso-SiO<sub>2</sub> was prepared using the reported method. The dry Meso-SiO<sub>2</sub>

---

<sup>a</sup> School of Materials Science and Engineering, Nanyang Technological University, 50 Nanyang Avenue, 639798, Singapore

<sup>b</sup> State Key Laboratory of Luminescent Materials and Devices, Institute of Polymer Optoelectronic Materials and Devices, South China University of Technology, Guangzhou, 510640, China

<sup>c</sup> Division of Physics and Applied Physics, School of Physical and Mathematical Sciences, Nanyang Technological University, 637371, Singapore

was immersed into perovskites solution. After a short time, the residue solution was removed, the powder was collected and dried on 120 °C for 30 min.

**WLED** was fabricated based on commercial UV LED (emission wavelength at 365 nm). Powders of perovskite implanted Meso-SiO<sub>2</sub> was pressed onto glass slide to form a flat palette. A thin layer of PMMA was coated on top of the palette to protect it from atmosphere. The glass slide was then covering the UV LED to produce white light.

### Characterizations

Thin film and powder X-ray diffraction (XRD) was carried out on Bruker D8 advance. Single crystal X-ray diffraction was undertaken using a Bruker SMART APEX-II system. The system uses a Mo sealed tube source along with a graphite monochromator to produce X-rays of wavelength 0.71073 Å. Bruker SAINT software package was used to collect and integrate X-ray intensity data using a narrow frame algorithm.<sup>2</sup> Multi-scan absorption corrections were applied using SADABS and the data symmetry was evaluated using XPREP.<sup>2</sup> Data was solved using SHELXT and refined on  $F^2$  using SHELXL in the program suite WinGX.<sup>3-5</sup> All images for publication were made using CrystalMaker.<sup>6</sup>

Absorption was obtained by using Agilent Cary 5000 UV-Vis-NIR. FTIR was measure on PerkinElmer Frontier. Static Photoluminescence spectra (PL) were measured with Ocean Optics Maya 2000 Pro spectrometer. The PL quantum yield was measured with the spectrometer coupled with an integrating sphere. Thin film sample on glass slides was put into integrating sphere and excited by 365 nm focused LED light. Emission was directed through optical fiber to the spectrometer. The setup was constantly calibrated by using a standard halogen light source (HL-3-INT-CAL, Ocean Optics). Transient photoluminescence was measured on FLS1000 Spectrometer. Transient absorption spectroscopy was measured on Helios Fire coupled with pulsed laser 330 nm. Temperature dependent PL was collected by combining the spectrometer with a liquid nitrogen cryostat. All measurements were conducted under ambient air except that the temperature dependent PL which was measured in cryostat maintained at high vacuum. The energy barrier ( $E_b$ ) between self-trapped exciton band to free exciton band was obtained by fitting the ratio of narrow emission intensity to broad emission intensity ( $R$ ) with  $1/T$  using the following equation:

$$\ln R = -\frac{E_b}{k_B T} + b$$

The coefficient of determination ( $R^2$ ) of the fitting was 0.978.

The TA measurements were performed by a pump–probe spectrometer (Ultrafast systems, Helios Fire). The fundamental laser pulse is generated by a Ti:sapphire amplifier (Coherent, Legend Elite, 800 nm, 40 fs, 1 kHz repetition rate). The fundamental pulse is split into two parts by a beam splitter. One part is sent to an optical parametric amplifier (OPA) (Light Conversion, TOPAS Prime). The OPA emitted 660 nm pulse is chopped at a frequency of 500 Hz and focuses on a BBO crystal to generate a 330 nm pulse for the pump. The other part of the fundamental pulse is focused into a sapphire crystal to generate a white-light continuum (320-660 nm) that is used as the probe. The probe pulses are delayed in time with respect to the pump pulses using a motorized translation stage mounted with a retroreflecting mirror. The pump and probe are

spatially overlapped on the surface of the sample. The size of the focused spot at the sample position for the probe and pump beams is around 50  $\mu\text{m}$  and 100  $\mu\text{m}$ , respectively. The total pump-photon fluence is 73  $\mu\text{J}/\text{cm}^2$  at the sample position.

The WLED was characterized by using the Maya 2000 Pro spectrometer coupled with a Keithley 2400 source meter. The spectrometer was calibrated by a standard halogen light source (HL-3-INT-CAL, Ocean Optics). The luminous flux was calculated with the build-in spectroscopic functions in Oceanview software.

### Material characterization

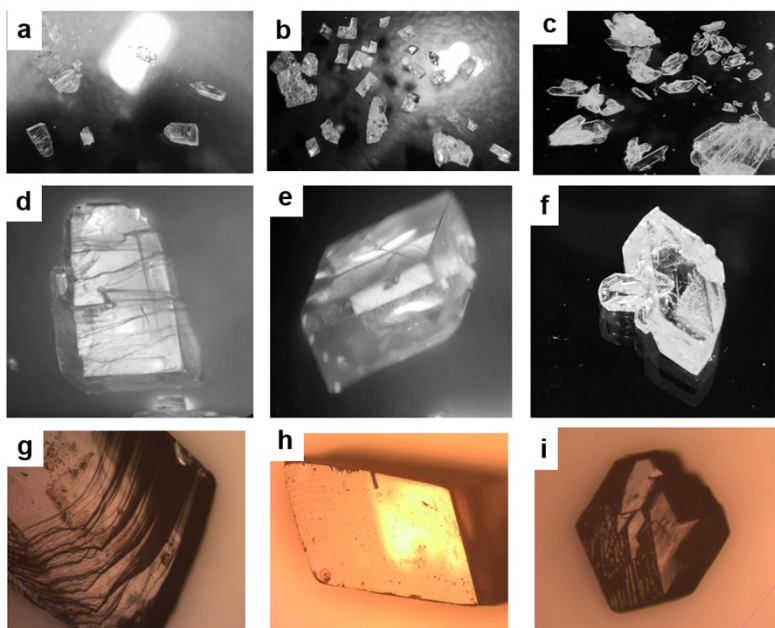


**Fig. S1** Photos and microscope images of the crystals of 2-MOP (a, d and g); 3-MOP (b, e and h); 4-MOP (c, f and i). The averaged crystal size is in millimeter range. The microscope images (g, h and i) shows the clean crystal facet and stacking of layers.

**Table S1.** Crystallographic data<sup>a</sup>

Empirical formula	$(\text{CH}_3\text{OC}_6\text{H}_4\text{CH}_2\text{NH}_3)_2\text{PbBr}_4$ (2-MOP)	$(\text{CH}_3\text{OC}_6\text{H}_4\text{CH}_2\text{NH}_3)_2\text{PbBr}_4$ (3-MOP)	$(\text{CH}_3\text{OC}_6\text{H}_4\text{CH}_2\text{NH}_3)_2\text{PbBr}_4$ (4-MOP)
formula weight	803.2	803.2	803.2
temperature	296(2) K	296(2) K	296(2) K
wavelength	0.71073 $\text{\AA}$	0.71073 $\text{\AA}$	0.71073 $\text{\AA}$

crystal system	monoclinic	monoclinic	monoclinic
space group	<i>P 21/c</i>	<i>P 21/c</i>	<i>P 21/c</i>
unit cell dimensions	$a = 16.9280(18) \text{ \AA}$ $\alpha = 90^\circ$ $b = 8.0054(9) \text{ \AA}$ $\beta = 98.742(5)^\circ$ $c = 8.5533(9) \text{ \AA}$ $\gamma = 90^\circ$	$a = 17.7662(10) \text{ \AA}$ $\alpha = 90^\circ$ $b = 8.0375(4) \text{ \AA}$ $\beta = 94.639(2)^\circ$ $c = 8.2585(5) \text{ \AA}$ $\gamma = 90^\circ$	$a = 17.1963(8) \text{ \AA}$ $\alpha = 90^\circ$ $b = 8.2080(3) \text{ \AA}$ $\beta = 104.152(3)^\circ$ $c = 8.4360(4) \text{ \AA}$ $\gamma = 90^\circ$
Volume	$1145.6(2) \text{ \AA}^3$	$1175.42(11) \text{ \AA}^3$	$1154.58(9) \text{ \AA}^3$
Z	4	4	4
R indices (all data)	$R1 = 0.0211$ $wR2 = 0.0498$	$R1 = 0.0235$ $wR2 = 0.0564$	$R1 = 0.0208$ $wR2 = 0.0473$

<sup>a</sup>Detailed crystallographic data can be seen in the cif files attached.

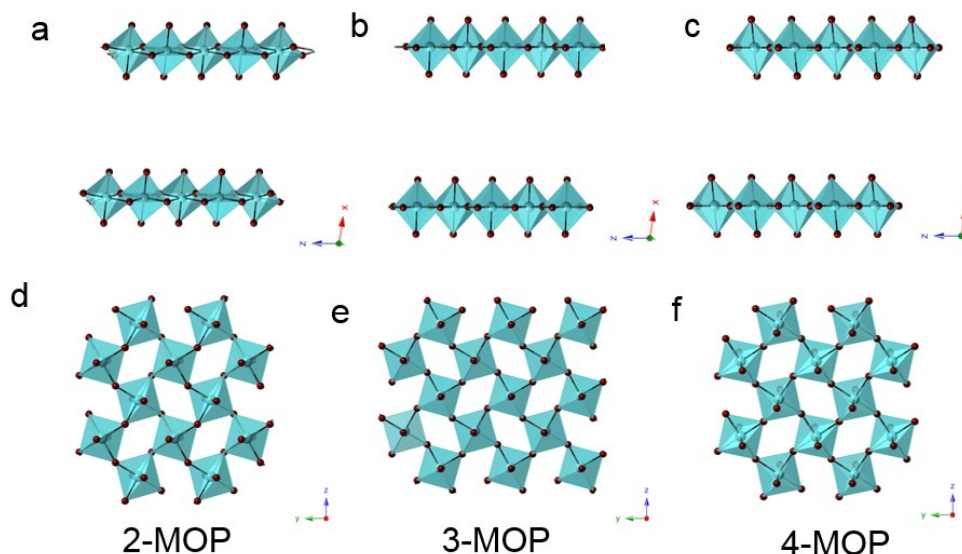
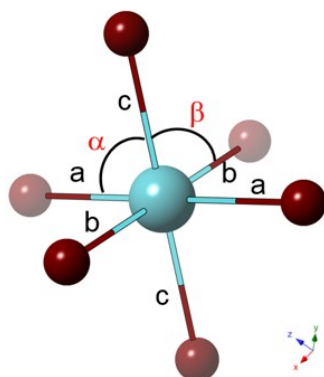


**Fig. S2** Structural overview of the perovskites. Out-of-plane view of the stacking of inorganic layers in 2-MOP, 3-MOP and 4-MOP (a, b and c); In plane view of the rotating octahedra (d, e and f).



Perovskites	a (Å)	b(Å)	c(Å)	$\Delta(\text{\AA})$	$\alpha$	$\beta$
2-MOP	3.06	3.05	2.99	0.036	87.97	87.64
3-MOP	2.99	2.99	2.99	0.006	85.72	89.41
4-MOP	3.02	2.99	3.00	0.009	89.73	83.26

**Fig. S3** Octahedra deformation in the perovskites. Parameter a and b are the bond length of Pb-( $\mu$ -Br), which functions to connect octahedra; c is the bond length of Pb-Br in the vertical

direction.  $\alpha$  and  $\beta$  are the angle of horizontal Pb-( $\mu$ -Br) bonds with vertical Pb-Br bond. Parameters are listed in the table. The deviations of bond length ( $\Delta$ ) are listed.

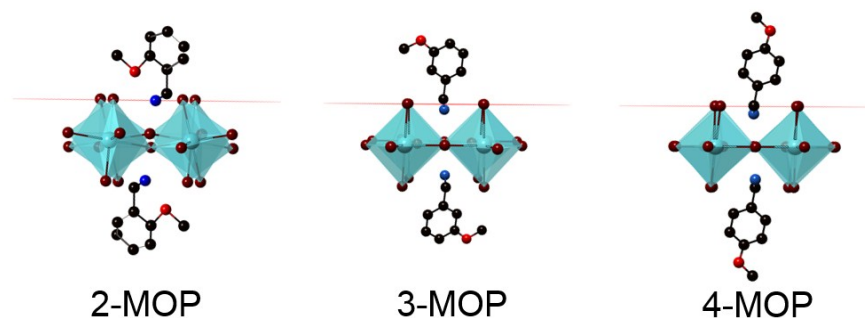


**Fig. S4** Intrusion of organic cations into planes formed with four terminal Br atoms. Intrusion depth for 2-MOP, 3-MOP and 4-MOP are 0 Å, 0.49 Å and 0.52 Å, respectively.

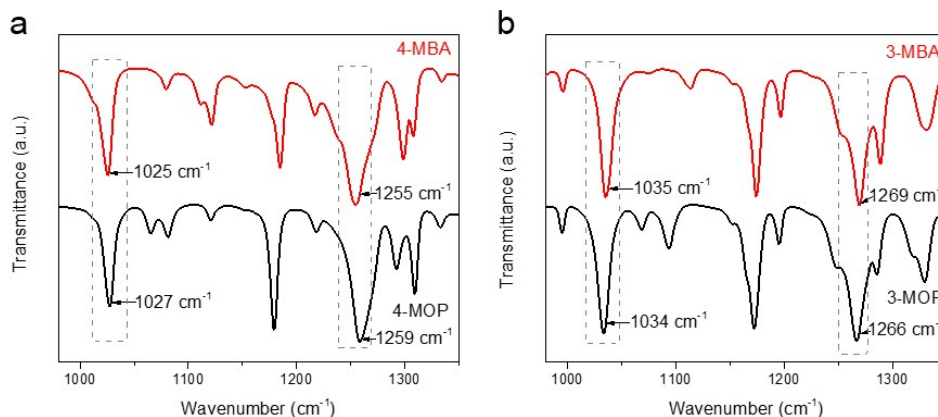


**Fig. S5** FTIR spectra of 4-MBA and 4-MOP (a); FTIR spectra of 3-MBA and 3-MOP (b).

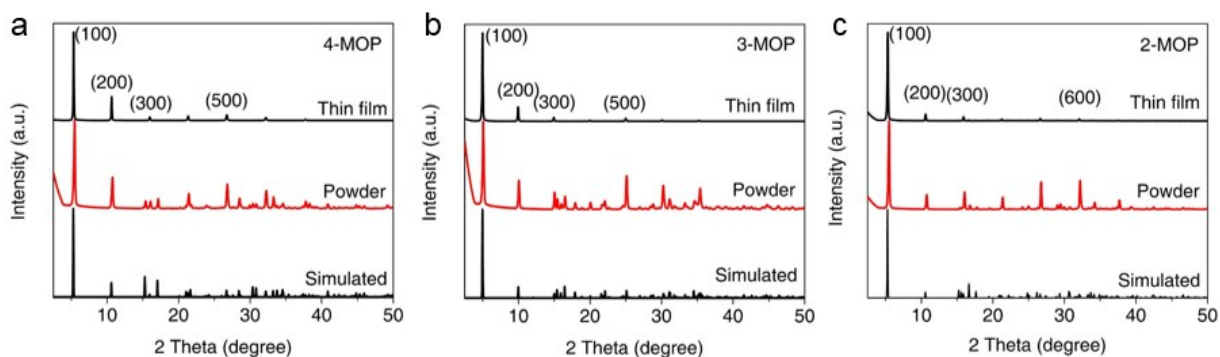


**Fig. S6** XRD patterns of 4-MOP (a), 3-MOP (b) and 2-MOP (c). Thin film and powder patterns are consistent with the simulated results.

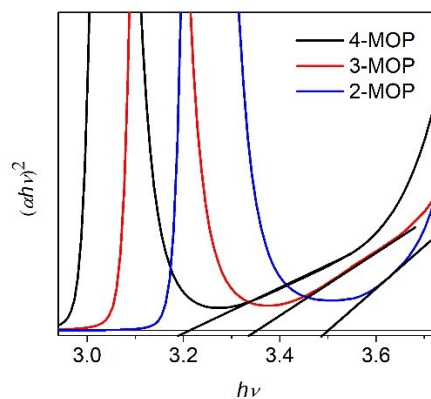


**Fig. S7** Optical bandgap ( $E_g$ ) derived from the absorption spectra. The  $E_g$  for 2-MOP, 3-MOP and 4-MOP are 3.5 eV, 3.36 eV and 3.22 eV, respectively. The exciton binding energy  $E_b$  was estimated from  $E_g - \text{PL}_{\text{max}}$ , where  $\text{PL}_{\text{max}}$  is the maxima of exciton emission. The energy level of free exciton (FE) was then calculated from  $E_g - E_b$ .

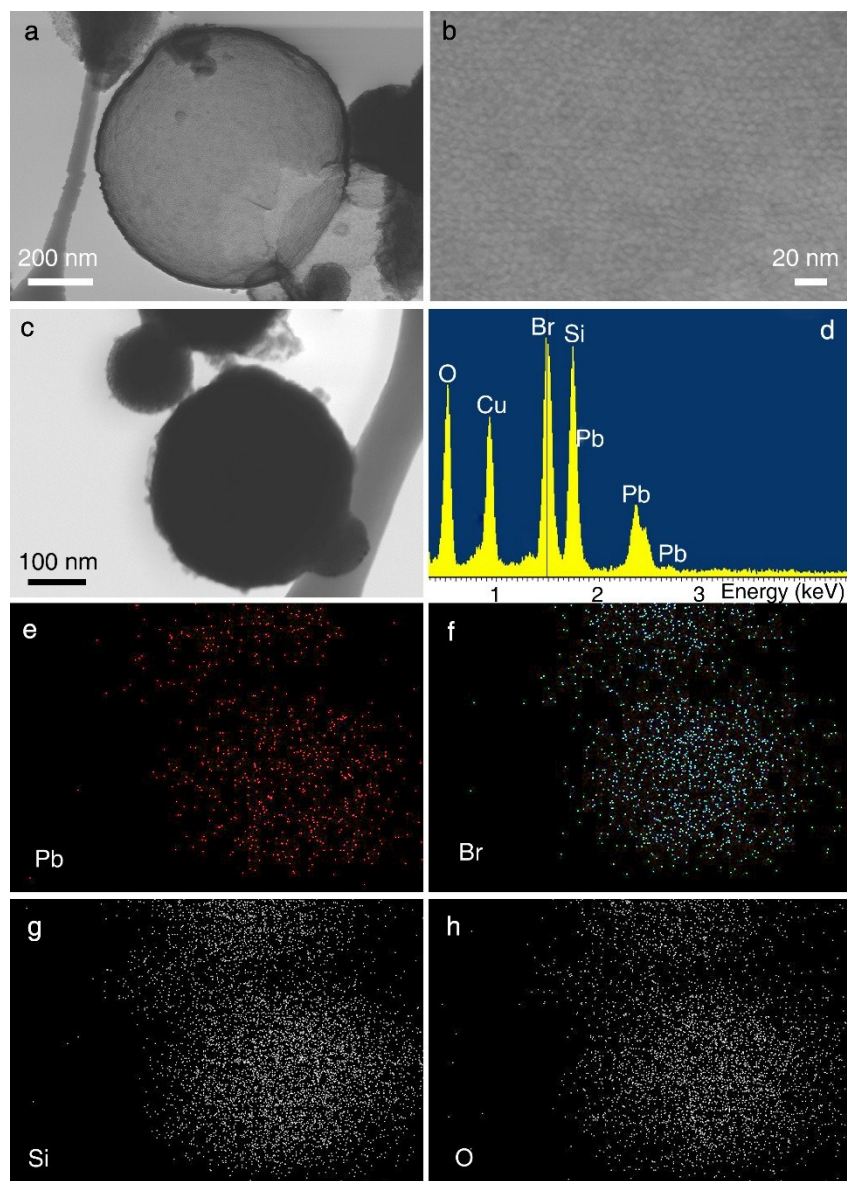


**Fig. S8** TEM images of meso-SiO<sub>2</sub> nanoparticle showing the hollow structure (a) and the magnified image shows the pore size below 10 nm (b). c, TEM image of the perovskite implanted meso-SiO<sub>2</sub> nanoparticle and its EDS spectrum; The EDS element mapping are shown in e, f, g, and h for Pb, Br, Si and O, respectively, showing the distribution of perovskites inside the mesopores.



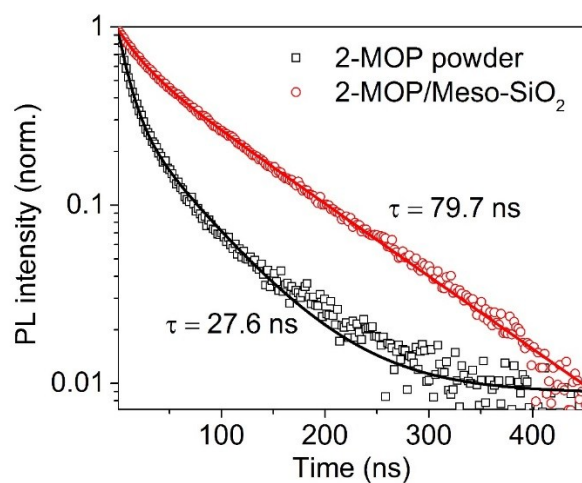


**Fig. S9** Photoluminescence decay of 2-MOP powder and 2-MOP/SiO<sub>2</sub>. The 2-MOP/SiO<sub>2</sub> shows longer emission lifetime ( $\tau = 79.7$  ns) than the 2-MOP powder ( $\tau = 27.6$  ns).

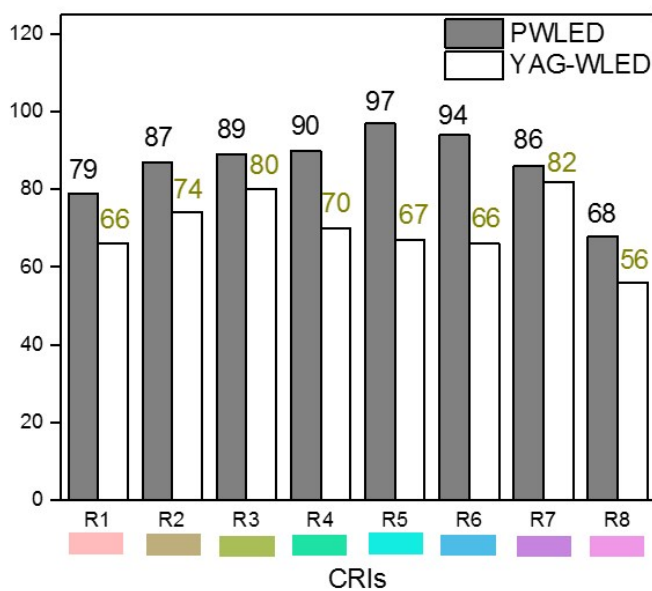


**Fig. S10** Color rendering index (CRIs) of PWLED and YAG-WLED. CIE R<sub>a</sub> was the average value of the eight CRIs. Daylight (D65) spectrum was used as the reference light source.



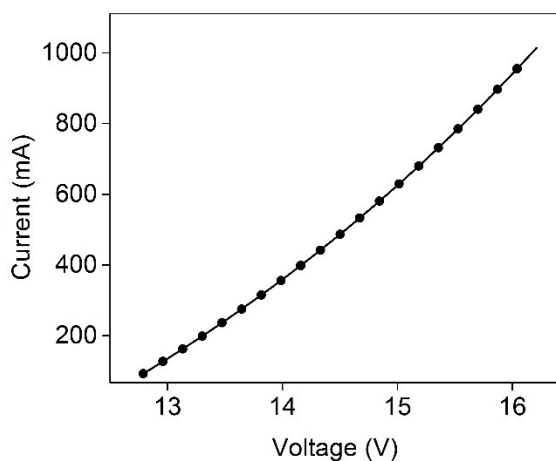


**Fig. S11** Driving voltage-current curve of the UV pumping light source.

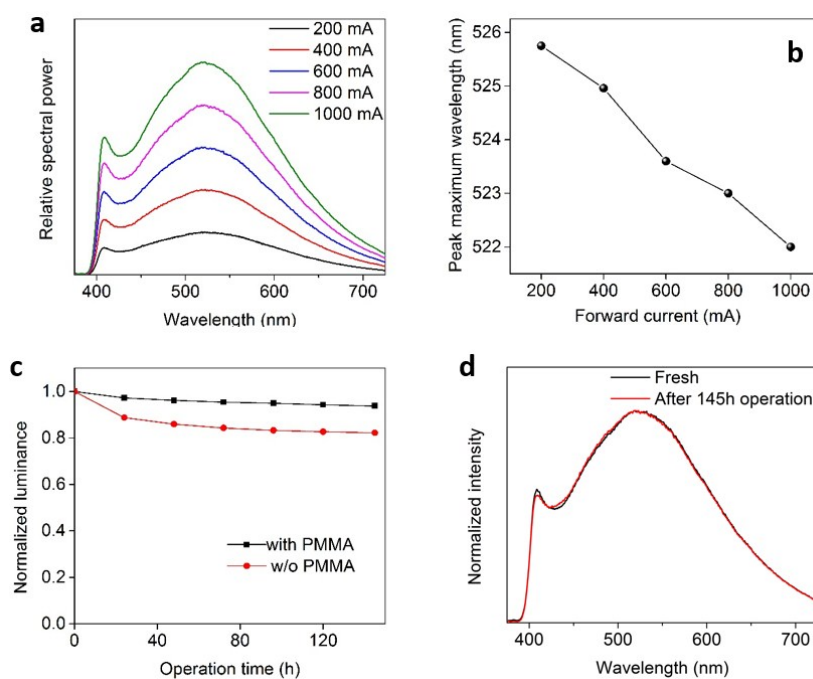


**Fig. S12** (a) Emission spectra of PWLED under varies driving current from 200 mA to 1000 mA; (b) The shift of peak maximum wavelength of the emission spectra under varies driving current; (c) Normalized luminance of PWLED with and without PMMA coating operated for 6 days; (d) Emission spectra of PWLED before and after operated for 145 h.

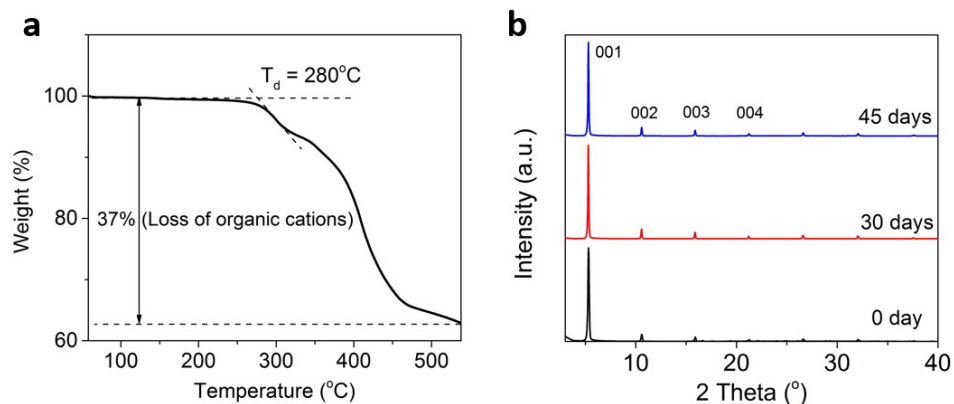


**Fig. S13** (a) Thermogravimetric curve of 2-MOP showing the decomposition temperature ( $T_d$ ) of 280°; (b) XRD patterns of 2-MOP exposed to ambient environment with a humidity of ~60% after 30 days and 45 days. The XRD patterns remain identical to the fresh sample.

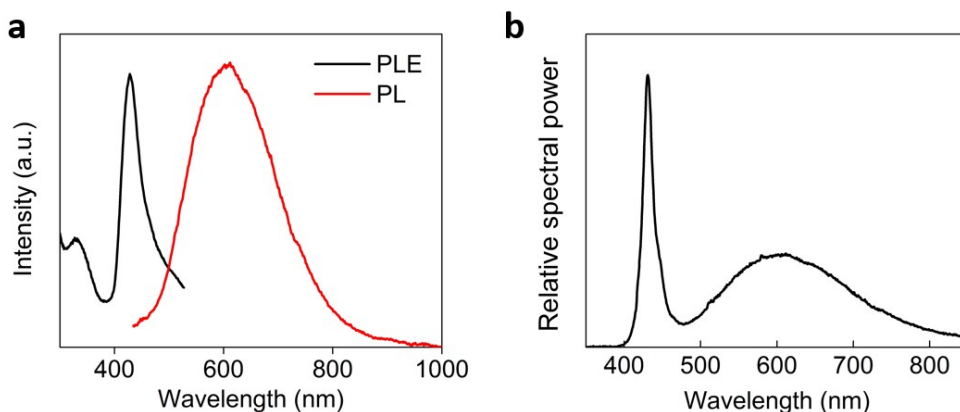


**Fig. S14** (a) Photoluminescence (PL) and photoluminescence excitation (PLE) spectra of 2-MBA based  $\text{PbI}_2$  perovskite; (b) Emission spectrum of a blue LED (430 nm) pumped perovskite composed from 2-MBA and  $\text{PbI}_2$ .

1. X. Wang, Y. Zhang, W. Luo, A. A. Elzatahry, X. Cheng, A. Alghamdi, A. M. Abdullah, Y. Deng and D. Zhao, *Chem. Mater.*, 2016, **28**, 2356–2362.
2. Bruker (2012). *SAINT, SADABS, XPREP*. Bruker AXS Inc., Madison, Wisconsin, USA. [Older versions (pre-1997) should refer to Siemens Analytical X-ray Instruments Inc. instead of Bruker AXS.]
3. G. M. Sheldrick, *Acta Cryst.*, 2015, **A71**, 3-8.
4. G. M. Sheldrick, *Acta Cryst.*, 2015, **C71**, 3-8.
5. L. J. Farrugia, *J. Appl. Cryst.*, 2012, **45**, 849-854.
6. D. C. Palmer, CrystalMaker, 2014, CrystalMaker Software Ltd, Begbroke, Oxfordshire, England.